AMERICAN SOCIETY FOR MICROBIOLOGY | Applied and Environmental Microbiology®

ENVIRONMENTAL MICROBIOLOGY

Enhancing the Adaptability of the Deep-Sea Bacterium *Shewanella piezotolerans* WP3 to High Pressure and Low Temperature by Experimental Evolution under H_2O_2 Stress

Zhe Xie,[a] Huahua Jian,[a] Zheng Jin,[a] Xiang Xiao[a,b,c]

[a]State Key Laboratory of Microbial Metabolism, School of Life Sciences and Biotechnology, Shanghai Jiao Tong University, Shanghai, China

[b]State Key Laboratory of Ocean Engineering, School of Naval Architecture, Ocean and Civil Engineering, Shanghai Jiao Tong University, Shanghai, China

[c]Laboratory for Marine Biology and Biotechnology, Qingdao National Laboratory for Marine Science and Technology, Qingdao, China

ABSTRACT Oxidative stresses commonly exist in natural environments, and microbes have developed a variety of defensive systems to counteract such events. Although increasing evidence has shown that high hydrostatic pressure (HHP) and low temperature (LT) induce antioxidant defense responses in cells, there is no direct evidence to prove the connection between antioxidant defense mechanisms and the adaptation of bacteria to HHP and LT. In this study, using the wild-type (WT) strain of a deep-sea bacterium, *Shewanella piezotolerans* WP3, as an ancestor, we obtained a mutant, OE100, with an enhanced antioxidant defense capacity by experimental evolution under H_2O_2 stress. Notably, OE100 exhibited better tolerance not only to H_2O_2 stress but also to HHP and LT (20 MPa and 4°C, respectively). Whole-genome sequencing identified a deletion mutation in the *oxyR* gene, which encodes the transcription factor that controls the oxidative stress response. Comparative transcriptome analysis showed that the genes associated with oxidative stress defense, anaerobic respiration, DNA repair, and the synthesis of flagella and bacteriophage were differentially expressed in OE100 compared with the WT at 20 MPa and 4°C. Genetic analysis of *oxyR* and *ccpA2* indicated that the OxyR-regulated cytochrome *c* peroxidase CcpA2 significantly contributed to the adaptation of WP3 to HHP and LT. Taken together, these results confirmed the inherent relationship between antioxidant defense mechanisms and the adaptation of a benthic microorganism to HHP and LT.

IMPORTANCE Oxidative stress exists in various niches, including the deep-sea ecosystem, which is an extreme environment with conditions of HHP and predominantly LT. Although previous studies have shown that HHP and LT induce antioxidant defense responses in cells, direct evidence to prove the connection between antioxidant defense mechanisms and the adaptation of bacteria to HHP and LT is lacking. In this work, using the deep-sea bacterium *Shewanella piezotolerans* WP3 as a model, we proved that enhancement of the adaptability of WP3 to HHP and LT can benefit from its antioxidant defense mechanism, which provided useful insight into the ecological roles of antioxidant genes in a benthic microorganism and contributed to an improved understanding of microbial adaptation strategies in deep-sea environments.

KEYWORDS *Shewanella*, deep sea, experimental evolution, high pressure, low temperature, oxidative stress, stress adaptation

Oxidative stresses commonly exist in natural environments, and microbes have developed a variety of defensive systems to counteract such events. HHP (high hydrostatic pressure) and LT (low temperature) are two of the most remarkable

Received 1 November 2017 **Accepted** 10 December 2017

Accepted manuscript posted online 21 December 2017

Citation Xie Z, Jian H, Jin Z, Xiao X. 2018. Enhancing the adaptability of the deep-sea bacterium *Shewanella piezotolerans* WP3 to high pressure and low temperature by experimental evolution under H_2O_2 stress. Appl Environ Microbiol 84:e02342-17. https://doi.org/10.1128/AEM.02342-17.

Editor Robert M. Kelly, North Carolina State University

Address correspondence to Xiang Xiao, xoxiang@sjtu.edu.cn.

characteristics of the majority of deep-sea environments (1). Both characteristics can affect cellular function by negatively influencing cell integrity, membrane fluidity, macromolecular interactions, and energy utilization, which can lead to metabolic disorders and redox imbalances (2, 3). As bacterial metabolism and cellular integrity are maintained by balancing the redox state of all cellular components for optimal overall function, the disturbance of this balance is accompanied by an increase in oxidative stress (4). For example, as reactive oxygen species (ROS) might come from the electron transport chain in the cell membrane, damage to the membrane caused by HHP could lead to the leakage of electrons, which can be intercepted by O_2 and form ROS. In *Shewanella benthica* KT99 and *Shewanella violacea* DSS12, a novel membrane-bound *ccb*-type quinol oxidase displaces the bc_1 complex and cytochrome *c* oxidase to overcome oxidative stress under HHP conditions. Moreover, LT could increase the solubility of oxygen and result in increased concentrations of ROS and, thus, the potential for oxidative damage (3). Therefore, bacteria living in such environments have to overcome oxidative stress.

Antioxidative genes/proteins are commonly found in marine extremophiles (5, 6). *S. violacea* DSS12, a psychrophilic facultative piezophile isolated from deep-sea sediments, has approximately 15 types of antioxidative genes. A cold-adapted bacterium, *Colwellia psychrerythraea* 34H, has been isolated from Arctic marine sediments and has approximately 13 types of antioxidative genes. A series of recent studies revealed that LT or HHP could lead to microbial oxidative stress responses and the expression of antioxidant enzymes. The transcription of the oxidative stress-related genes *ahpC*, *katG*, *oxyR*, *soxS*, *sodA*, *sodC*, and *grxA* was found to be significantly induced in *Salmonella enterica* serovar Typhimurium in response to cold stress (5°C) (7). Proteomic analysis of the responses of *Lactococcus piscium* CNCM I-4031 to cold stress showed that two antioxidant proteins, Ahp and thioredoxin (Trx), were induced (8). Treatment of *Escherichia coli* O157:H7 with HHP (100 MPa) resulted in upregulated transcription levels of the antioxidative genes *trxA*, *trxC*, and *grxA*. *dps*, *trxA*, and *trxB* mutants of *E. coli* K-12 were shown to be significantly more sensitive to HHP (400 MPa) than their wild-type (WT) counterparts (9). In addition, *E. coli* MG1655 mutants lacking ROS scavengers (KatE, KatF, SodAB, and SoxS) were also found to be more pressure sensitive than the wild-type strains (10). Moreover, a radioresistant bacterium, *Deinococcus radiodurans* R1, which can resist oxidative stress, was also found to be highly piezo resistant (11). All of those studies indicated that antioxidation might play a role in HHP and LT adaptation. In *Saccharomyces cerevisiae*, it has been proven that enhanced oxidative stress tolerance leads to enhanced tolerance to HHP stress (12). However, whether bacteria with increasing antioxidant defense capacities would better adapt to double stresses of HHP and LT remains unknown.

Shewanella strains are among the most abundant *Proteobacteria* in the deep-sea environment. *Shewanella piezotolerans* WP3 (here referred to as WP3) was isolated from West Pacific sediments at a depth of 1,914 m, where the *in situ* temperature is ~2°C and the hydrostatic pressure is 20 MPa (13). In this study, the associations of antioxidants with adaptation to HHP and LT were investigated by developing an evolved strain, OE100, which was cultured with a challenge concentration of H_2O_2. Remarkably, OE100 exhibited increased H_2O_2 tolerance and simultaneously better growth at 20 MPa and 4°C. Resequencing of the genome revealed that deletion mutations occurred in a key oxidative stress response transcriptional regulator, OxyR, and two polar flagellar genes. Transcriptional analysis revealed that the genes associated with oxidative stress defense, anaerobic respiration, DNA repair, and the synthesis of flagella and bacteriophage were differentially expressed in OE100 compared with the WT at 20 MPa and 4°C. Through the construction of an OxyR in-frame deletion strain (Δ*oxyR*c), we confirmed that reduced OxyR levels could contribute to the adaptation of WP3 to HHP and LT. Taken together, the results of our study suggest that oxidative stress defense is a common adaptation strategy for bacteria coping with cold deep-sea environments.

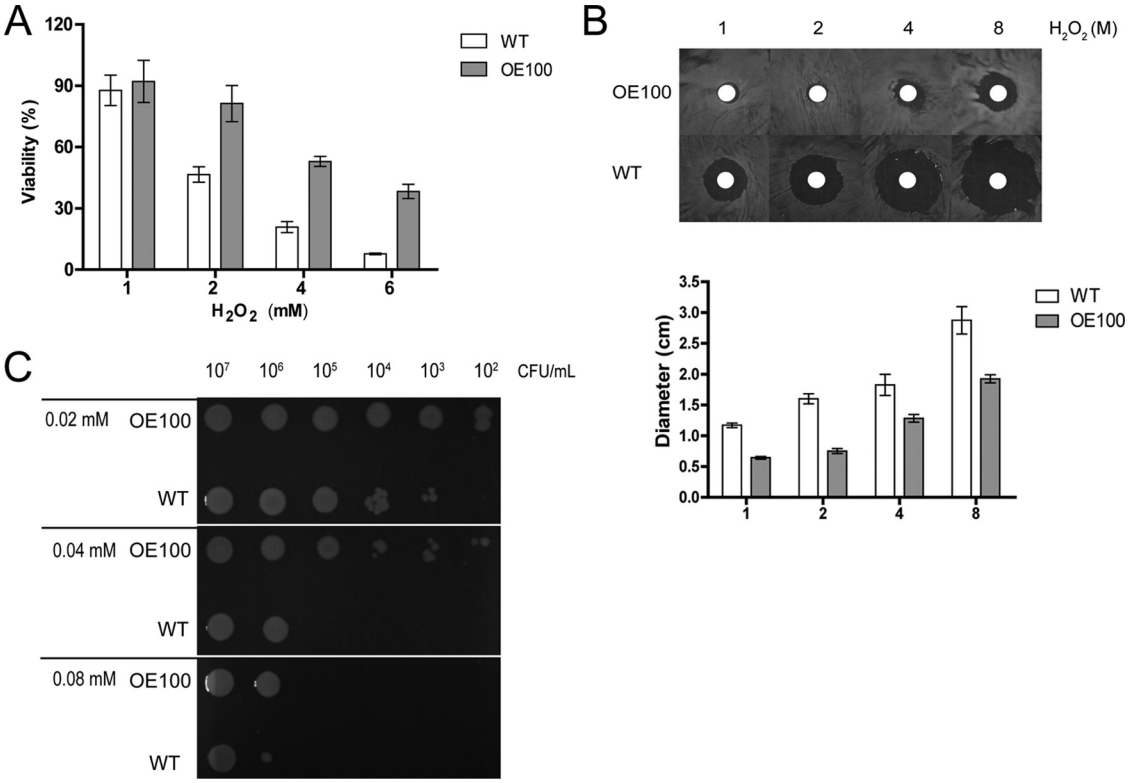

FIG 1 Characteristics of OE100 in response to H_2O_2 stress. (A) Survival assay. H_2O_2 was added to mid-log-phase cultures to the final concentrations indicated. After 20 min, the samples were properly diluted and plated onto 2216E plates. Colony counting was performed after 48 h. (B) Disc diffusion assay. Paper discs loaded with 10 μl H_2O_2 at different concentrations were placed onto bacterial lawns (grown for 8 h). The results shown are from 48 h after the discs were in place. For data presentation, the sensitivity of each strain was calculated by its average diameter ($n = 4$). Error bars represent standard deviations. (C) Plating defect assay. Mid-log-phase cultures were adjusted to 10^8 CFU/ml and diluted by 10-fold series dilutions, and 5 μl of each dilution was plated onto 2216E plates with H_2O_2 added at different concentrations. Images were captured 48 h after plating. All experiments were performed three times, and similar results were obtained.

RESULTS

Obtaining the H_2O_2-tolerant WP3 strain by experimental evolution. Six bacterial populations of the WP3 wild-type strain were evolved under H_2O_2 stress as described in Materials and Methods. After 500 generations of growth, 6 single-colony isolates, named E1-1, E2-1, E3-1, E4-1, E5-1, and E6-1, from each evolved population were randomly picked by plating and single-colony isolation. Among the six strains, E6-1 had the highest endpoint culture density (optical density at 600 nm [OD_{600}] of 4.7; $P < 0.05$) in medium with 0.6 mM H_2O_2 (see Fig. S1 in the supplemental material). This strain was named OE100 and selected for follow-up analysis.

The tolerance of evolved strain OE100 to H_2O_2 is significantly increased. To compare the levels of H_2O_2 tolerance of OE100 and the WT, viability assays, disc diffusion assays, and plating defect assays were performed. Although there was no significant difference in viability between OE100 and the WT with a low H_2O_2 concentration (1 mM), OE100 showed a higher survival rate than that of the WT when the H_2O_2 concentration was increased from 1 mM to 6 mM. When the H_2O_2 concentration was 6 mM, the survival rate of OE100 was approximately 5 times higher than that of the WT (Fig. 1A). Moreover, the disc diffusion assay showed that the diameter of the inhibition zone of OE100 was smaller than that of the WT, indicating that OE100 has a greater ability to resist H_2O_2 stress than the WT (Fig. 1B). In addition, the viability of the OE100 strain was significantly improved, as demonstrated by plating defect assays (Fig. 1C). All of these data collectively led to the conclusion that OE100 was more resistant to H_2O_2 than its ancestor WT strain, indicating that the antioxidation property of OE100 was significantly increased during the experimental evolution process.

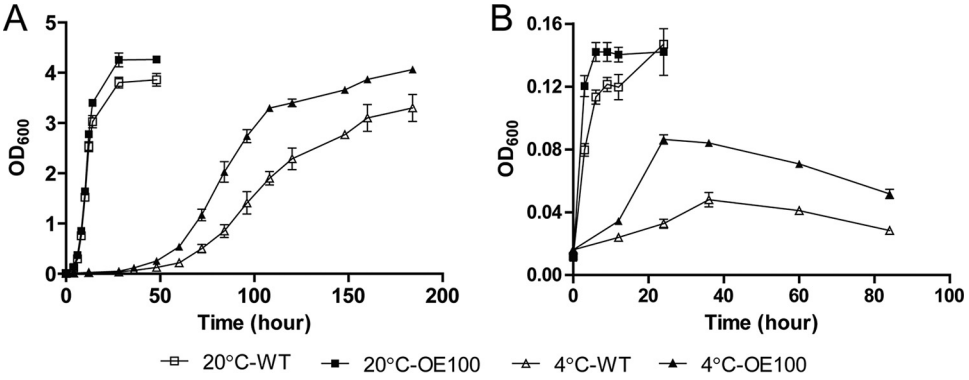

FIG 2 Growth curve of OE100 in 2216E medium at different temperatures and pressures. (A) Growth of OE100 at 0.1 MPa and different temperatures. (B) Growth of OE100 at 20 MPa and different temperatures. The average values and standard deviations, displayed by the error bars, resulted from three replicates. All of the data shown represent results from at least three independent experiments.

OE100 shows better growth at 4°C and 20 MPa. To test whether the increase in the antioxidant defense capacity can enhance the adaptability of the WT to HHP and LT, the growth of OE100 at different pressures and temperatures was examined. Under ambient pressure conditions (0.1 MPa), OE100 exhibited a higher growth yield than that of the WT at both 20°C and 4°C (Fig. 2A). A similar result was obtained when OE100 was cultured at high pressure. The growth rates of OE100 and the WT were 0.08 h^{-1} and 0.06 h^{-1}, respectively, and OE100 showed a significantly higher cell density than that of the WT at 4°C and 20 MPa (Fig. 2B), which are the *in situ* temperature and hydrostatic pressure in locations inhabited by WP3.

Genomic changes and natures of mutated genes. To identify the genetic basis of the increased fitness of the evolved strain under HHP and LT conditions, the genomes of H_2O_2-evolved strain OE100 and the ancestral WT strain were sequenced, and the data were analyzed. We obtained 90,393 subreads with 173× coverage of the WT genome and 181,030 subreads with 213× coverage of the OE100 genome. The genomic sequence of OE100 differed from the ancestral WT sequence by 5 deletions (Table 1) and 7 single-nucleotide polymorphisms (SNPs) (Table 2).

Interestingly, only one of the sequenced mutations occurred in a gene with a well-known role in the oxidative stress response. A 69-bp deletion occurred in the oxidative stress transcriptional regulator gene *oxyR*. OxyR features a sensory cysteine residue that is directly oxidized by H_2O_2, thereby generating a disulfide bond that alters its binding to DNA and controls the transcription of H_2O_2 scavenger genes (14). We confirmed that the reduced amino acid sequence of OxyR in OE100 belonged to the C-terminal substrate-binding domain containing these two conserved cysteine residues (Cys203 and Cys212 in WP3 OxyR are homologous to the Cys199 and Cys208 in *E. coli* OxyR) (see Fig. S2 in the supplemental material).

In addition, a 1,899-bp deletion was located within the coding region of two *fliC1* genes (encoding polar flagellin). The swimming motility assay with OE100 showed that the deletion in *fliC1* led to a significant decrease in the swimming ability (Fig. S3). Moreover, a single-base deletion and a 12-bp deletion in two separate genes of

TABLE 1 Deletions present in OE100 compared to the WT

Gene	Position on genome	Annotated function	Length of deletion (bp)
SWP_RS16075	3815802	Hypothetical protein	1
SWP_RS09080	2105025	Hypothetical protein	12
oxyR	4012375	Transcriptional regulator, LysR family OxyR	69
$fliC1_a$	1555674	FliC, polar flagellin domain protein	70
$fliC1_b$	1556355	FliC, polar flagellin domain protein	1,215

TABLE 2 SNPs present in OE100 compared to the WT

Gene	Position on genome	Annotated function	Type of amino acid change (amino acid change)	Nucleotide change
trkH	56774	K^+ transporter Trk	Silent (S483S)	G→A
23S rRNA	76729	23S rRNA		T→C
yjjW	228972	Pyruvate formate lyase-activating enzyme	Missense (H42Q)	C→G
acrR	244302	TetR family transcriptional regulator	Silent (L84L)	C→T
rpoD	1115319	RpoD RNA polymerase sigma factor 70	Missense (A273G)	C→G
SWP_RS13360	3125851	Hypothetical protein	Nonsense (Q464Stop)	T→C
tauE	4099249	Cytochrome *c* biogenesis	Silent (A326A)	A→C

unknown function (Table 1) indicated the previously unrecognized mechanisms of the oxidative stress response and adaptation under experimental conditions.

SNPs were located within the coding regions of six genes (*trkH*, 23S rRNA, *yjjW*, *acrR*, *rpoD*, and *tauE*) with annotated functions and in one gene of unknown function (SWP_RS13360) (Table 2); no mutations were found in the noncoding or intergenic regions. Among these SNPs, there are only two missense mutations (*yjjW* and *rpoD*) and one nonsense mutation (SWP_RS13360). The *yjjW* gene encodes a glycine radical enzyme activase that acts on a wide variety of biomolecules in numerous pathways, including vitamin biosynthesis and coenzyme biosynthesis (15). The *rpoD* gene encodes a σ^{70} protein that can affect the expression state of cells (16). Therefore, mutations in these two genes could rewire the network into a more efficient state and affect the fitness of OE100.

Transcriptomic changes in OE100 compared to the WT. To check the contribution of the other transcriptional rearrangements to the increased fitness of OE100 at HHP and LT, differentially expressed genes between the WT and OE100 at maximum growth yields at 20 MPa and 4°C were investigated by whole-genome transcriptional analysis. To validate the transcriptome sequencing (RNA-Seq) data, 9 genes, including those that were upregulated, downregulated, or unchanged, were selected for reverse transcription (RT)-quantitative PCR (qPCR). The relative mRNA levels for each gene were calculated and log transformed. The correlation coefficient (R^2) between the data obtained by microarray analysis and those obtained by qPCR was 0.9213, demonstrating that the transcriptome data were reliable and could be used for the follow-up analysis (see Fig. S4 in the supplemental material).

Compared to the WT, 483 genes (approximately 10% of the WP3 genome) in OE100 showed significant differential expression ($\log_2$ fold change for OE100 compared to the WT of $\geq$1; *P* value [false discovery rate {FDR}] of $<$0.001), of which 302 genes and 181 genes were up- and downregulated, respectively (Fig. S5). Specifically, the transcription levels of most genes encoding the scavenger enzymes involved in hydrogen peroxide or peroxide elimination were upregulated (Table 3). For example, *katE* and *ahpC*, which are genes that encode the primary H_2O_2 scavengers in many bacteria, showed 4-fold- and 32-fold-higher expression levels in OE100 than in the WT, respectively. *ccpA2* and *gpx*, which are also responsible for H_2O_2 scavenging, were upregulated by 1.6-fold and 3.6-fold, respectively. In addition, the transcription level of *dps*, which is a homologue of the *dps* gene in *E. coli* with both the "ferritin-like" activity and the DNA-binding capacity, was upregulated by 1.68-fold. However, the transcription levels of the genes involved in superoxide scavenging (*sod*) were not significantly different.

In addition, most of the genes related to anaerobic respiration on different electron acceptors, including nitrate, nitrite, fumarate, and dimethyl sulfoxide (DMSO), showed significant upregulation in OE100, while the genes related to the aerobic electron transport chain were downregulated. CymA, a cytoplasmic-membrane-bound *c*-type cytochrome belonging to the NapC/NirT protein family that directs electrons from the menaquinol pool to the periplasm, was induced by 1.7-fold in OE100. This protein was proven to be the essential electron transport protein for the anaerobic respiratory flexibility of the *Shewanellae* (17). In WP3, CymA is involved in the reduction of nitrate, nitrite, DMSO, and fumarate, and it was proven to serve as the sole electron transporter

TABLE 3 Selected differentially expressed genes in OE100 at 4°C and 20 MPa (probability > 0.8)

Function	Gene	Gene description[a]	Log_2 fold change (OE100/WT)
Antioxidant activity	SWP_RS05640	Glutathione peroxidase Gpx	1.85
	SWP_RS16945	Transcriptional regulator OxyR	1.55
	SWP_RS00790	DNA-binding protein Dps	0.75
	SWP_RS19255	Transcriptional regulator OhrR	1.80
	SWP_RS19285	Alkyl hydroperoxide reductase subunit F, AhpF	1.24
	SWP_RS19290	Alkyl hydroperoxide reductase subunit C, AhpC4	1.62
	SWP_RS19745	Catalase KatE	2.05
	SWP_RS12910	Cytochrome *c* peroxidase CcpA2	0.69
Nitrate respiration	SWP_RS19850	Anaerobic dehydrogenases NapAβ	1.86
	SWP_RS19855	Nitrate reductase NapBβ	1.95
	SWP_RS19845	Periplasmic nitrate reductase NapDβ	1.69
Nitrite respiration	SWP_RS20710	Formate-dependent nitrite reductase, NrfC protein	6.50
	SWP_RS20715	Formate-dependent nitrite reductase, NrfG protein	7.07
	SWP_RS20705	Formate-dependent nitrite reductase, NrfD protein	5.87
	SWP_RS17675	Nitrite reductase	1.92
Anaerobic respiration	SWP_RS21330	Membrane-bound tetraheme cytochrome *c* CymA	0.78
Fumarate respiration	SWP_RS01965	Fumarate reductase cytochrome *b* subunit	1.69
	SWP_RS01970	Fumarate reductase respiratory complex subunit	1.82
	SWP_RS01975	Fumarate reductase flavoprotein subunit	1.60
	SWP_RS01980	Succinate dehydrogenase/fumarate reductase iron-sulfur protein	1.58
DMSO respiration	SWP_RS03195	Decaheme cytochrome *c* CytC	1.98
	SWP_RS03200	Transcriptional regulator, LysR family, LysR2	1.65
	SWP_RS03205	Twin-arginine translocation pathway signal, DmsA2	1.98
	SWP_RS03215	Cytoplasmic chaperone TorD	1.73
	SWP_RS03210	4Fe-4S ferredoxin, iron-sulfur binding	1.82
	SWP_RS03220	Hypothetical protein	1.37
	SWP_RS15435	Conserved hypothetical protein DmsH	1.16
Polar flagellum	SWP_RS06720	Flagellin FlaG1	1.89
	SWP_RS06655	Flagellar basal body rod protein FlgB1	1.33
	SWP_RS06660	Flagellar basal body rod protein FlgC1	1.23
	SWP_RS06775	ATPase FliI/YscN	−1.02
	SWP_RS06690	Flagellar P-ring protein	−1.03
	SWP_RS06770	Flagellar assembly protein FliH1	−1.17
	SWP_RS06780	Flagellar protein FliJ1	−1.34
	SWP_RS06715	Flagellin, $FliC1_b$	−3.07
Lateral flagella	SWP_RS22555	Sodium-type flagellar protein MotY	1.83
	SWP_RS22550	Motor switch part FliM	1.39
	SWP_RS22700	Flagellin, FliC2	−3.82
Phage	SWP_RS11565	Putative capsid protein FpsC	−5.58
	SWP_RS11550	Minor capsid protein FpsD	−9.92
	SWP_RS11570	Zonula occludens toxin FpsH	−5.47
	SWP_RS11545	ssDNA-binding protein FpsB	−9.32
	SWP_RS11560	Minor capsid protein FpsF	−6.31
	SWP_RS11535	Transcription regulator FpsR	−6.31
	SWP_RS11540	Replication protein FpsA	−11.22
DNA repair	SWP_RS05950	DNA repair protein RecN	−2.35
	SWP_RS23035	DNA polymerase ImuA	−3.04
	SWP_RS10395	DNA polymerase ImuB	−2.79
	SWP_RS10400	DNA polymerase V DnaE2	−2.47
	SWP_RS05205	DNA polymerase IV	−3.02
	SWP_RS21400	Peptidase S24, LexA repressor	−2.04
	SWP_RS06045	DNA recombination/repair protein RecA	−0.87
	SWP_RS20905	MutT/nudix family protein	−1.99

[a]ssDNA, single-stranded DNA.

toward nitrite reductase (18). Moreover, compared to other anaerobic respiration pathways, nitrite reductases have the highest expression levels (*nrfC*, 89-fold; *nrfG*, 134-fold; *nrfD*, 58-fold).

Most of the genes involved in flagellar biosynthesis, phage production, and DNA repair were repressed (Table 3). The genes encoding polar flagellin (*fliC1*$_b$) and lateral flagellin (*fliC2*) were downregulated by 8.4-fold and 14-fold, respectively. The genes encoding filamentous phage capsid proteins (FpsC, FpsD, and FpsF) were significantly downregulated by 47.8-fold, 968.7-fold, and 79.3-fold, respectively. The expression level of DNA polymerase IV, which is a translesion polymerase known to promote damaged DNA survival by allowing replication to bypass lesions, was decreased by 8.1-fold. In addition, the transcription levels of two key genes involved in the SOS response, *lexA* and *recA*, were repressed by 4.1-fold and 1.8-fold, respectively.

Deletion mutation of *oxyR* results in increased growth of WP3 at 20 MPa and 4°C. There was a 69-bp deletion located in the C-terminal substrate-binding domain of *oxyR* in OE100. To confirm whether the reduced level of the *oxyR* gene was involved in LT and HHP adaptation, an OxyR in-frame deletion strain (Δ*oxyR*c) with an identical 69-bp deletion was constructed based on WP3Δ4RE, which was a wild-type WP3 strain with 4 restriction enzyme gene deletions and a higher conjugation efficiency (19). The Δ*oxyR*c strain carrying pSW2 showed a higher tolerance to H_2O_2 than did WP3Δ4RE/pSW2, and this phenotype was abolished in the Δ*oxyR*c/*oxyR* strain (complementation of the Δ*oxyR*c strain with the *oxyR* gene) (Fig. 3A), suggesting that the mutation in OxyR was responsible for the phenotype. Notably, the Δ*oxyR*c strain carrying pSW2 demonstrated better growth at 20 MPa and 4°C, indicating that reduced *oxyR* levels in OE100 contributed to the growth of OE100 at 20 MPa and 4°C (Fig. 3B). Interestingly, out of 30 single-colony isolates that were randomly picked from 6 evolved populations (5 single-colony isolates from each evolved population), 19 strains were found to harbor the same deleted region in *oxyR* as the one present in OE100 (see Table S2 in the supplemental material), indicating that the mutation of this region in *oxyR* is important for WP3 survival under H_2O_2 stress.

As OxyR regulates different kinds of antioxidant genes, to identify the OxyR-regulated genes involved in adaptation to HHP and LT, the relative mRNA levels of these genes in the Δ*oxyR*c strain carrying pSW2 at 20 MPa and 4°C were examined by RT-qPCR (Fig. 3C). The transcription of the *oxyR* gene was upregulated in the Δ*oxyR*c strain carrying pSW2, suggesting that self-repression is present in *oxyR* expression. Expectedly, the transcriptions of the *katE*, *ahpF*, and *ahpC4* genes were significantly upregulated in the Δ*oxyR*c strain carrying pSW2 and downregulated in the Δ*oxyR*c/*oxyR* strain, indicating that OxyR in WP3 acts as a repressor of the *katE*, *ahpF*, and *ahpC4* genes, and the absence of a conserved domain stimulates the expression of these genes. Notably, the transcription of the *ccpA2* gene was upregulated in both the Δ*oxyR*c strain carrying pSW2 and the Δ*oxyR*c/*oxyR* mutant, thus demonstrating a similar pattern of change with *oxyR* and suggesting that OxyR acts as an activator of the *ccpA2* gene. Accordingly, the Δ*oxyR*c/*oxyR* mutant with a significantly high level of expression of the *ccpA2* gene also demonstrated better growth at 20 MPa and 4°C (Fig. 3B), indicating that the *ccpA2* gene was important for adaptation to HHP and LT. To test this notion, we constructed *ccpA2* deletion (Δ*ccpA2*/pSW2), complementation (Δ*ccpA2*/*ccpA2*), and overexpression (WT strain carrying *ccpA2*) mutants. Compared to the WT, the Δ*ccpA2* strain carrying pSW2 showed decreased growth at HHP and LT, while growth was increased in the Δ*ccpA2*/*ccpA2* strain and in the WT strain carrying *ccpA2* (Fig. 3D). Moreover, the Δ*ccpA2* strain carrying pSW2 did not show a growth defect at 0.1 MPa and 20°C (Fig. S6), suggesting that *ccpA2* is the major antioxidant facilitating the adaptation of WP3 to HHP and LT.

DISCUSSION

Based on our results, we have proposed a model to explain the enhanced HHP/LT adaptation mechanism of OE100 (Fig. 4). The most important system that contributes to adaptation to HHP and LT is an antioxidant defense system. As the substrate-binding

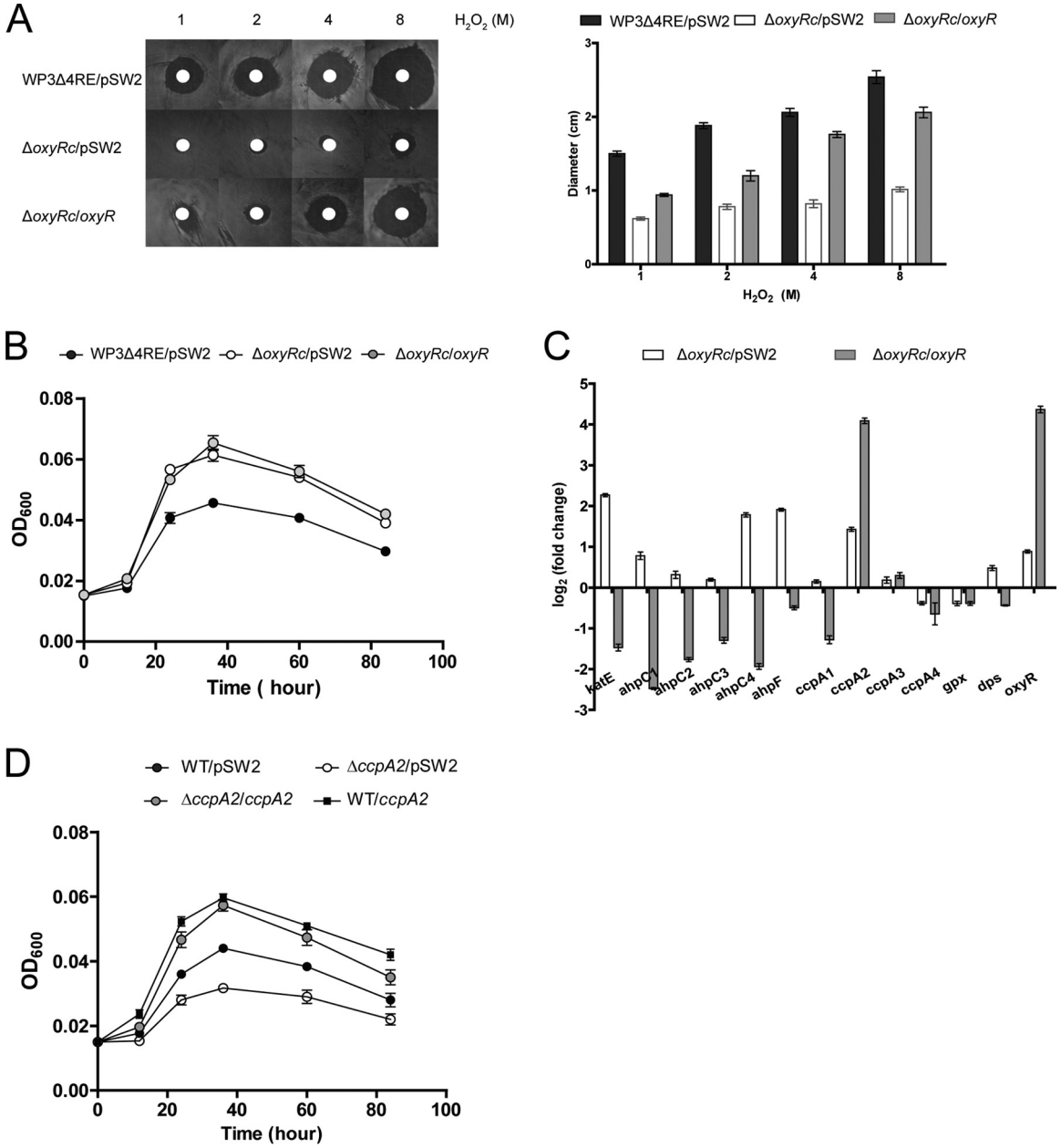

FIG 3 Characteristics of the Δ*oxyR*c strain. (A) Disc diffusion assay of the Δ*oxyR*c strain carrying pSW2 and the Δ*oxyR*c/*oxyR* strain in response to H_2O_2. (B) Growth curves of the Δ*oxyR*c strain carrying pSW2 and the Δ*oxyR*c/*oxyR* strain at 20 MPa and 4°C. (C) Impact of reduced OxyR levels on expression levels of various H_2O_2-scavenging genes. The expression levels of these genes in the Δ*oxyR*c strain carrying pSW2 and the Δ*oxyR*c/*oxyR* strain were normalized relative to those in WP3Δ4RE/pSW2. (D) Impact of the *ccpA2* gene on the growth of WP3 at 20 MPa and 4°C. All experiments were performed three times, and similar results were obtained.

domain of *oxyR* in OE100 was mutated, we inferred that OxyR lost the ability to sense H_2O_2 and affect its binding to target sites. OE100 showed greater resistance to H_2O_2, indicating that OxyR in OE100 functioned as a repressor for H_2O_2 scavenger genes, and the mutation of *oxyR* derepressed the expression of these genes. Through the construction of the Δ*oxyR*c mutant, we found that the Δ*oxyR*c mutant demonstrated better adaptation to HHP and LT with an increased antioxidant ability, indicating that antioxidation indeed contributes to adaptation to HHP and LT. The upregulated genes *katE*, *ahpF*, *ahpC4*, and *ccpA2* in the Δ*oxyR*c strain were also found to be induced in OE100 at 20 MPa and 4°C, suggesting that these genes were under the control of OxyR and contribute to adaptation to HHP and LT. Complementation with OxyR did not restore

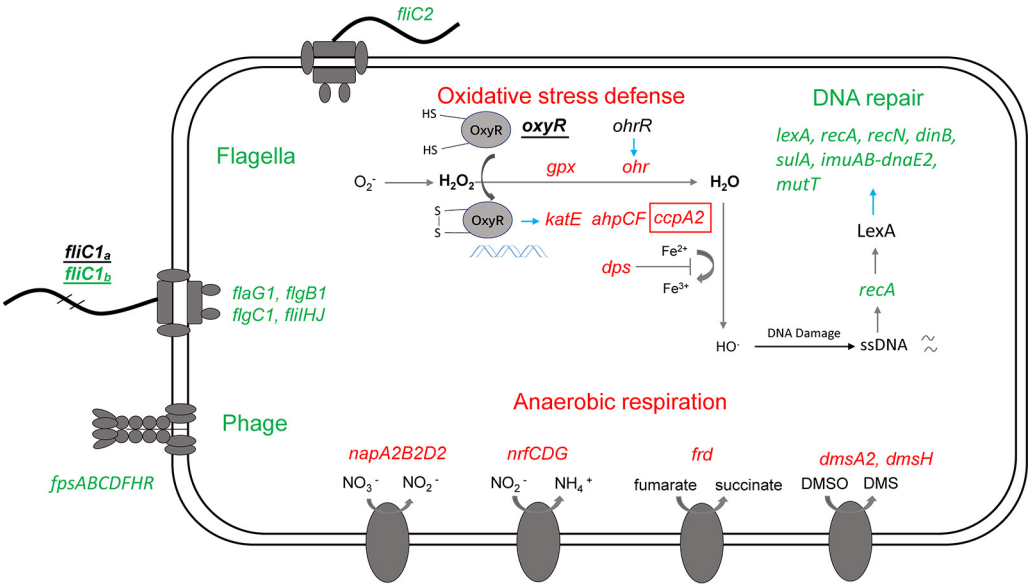

FIG 4 Graphic display of transcriptomic data for genes categorized by function in OE100 at 20 MPa and 4°C. Green and red indicate the genes that are induced and repressed (OE100/WT), respectively. Underlining indicates that the gene is mutated in OE100. Blue arrows represent gene regulation. The red rectangle indicates that the gene is important for adaptation to HHP and LT. DMS, dimethyl sulfide.

the wild-type phenotype at 20 MPa and 4°C. Previously, the copy numbers of pSW2 in WP3 were determined (12 and 30 copies at 20°C and 4°C, respectively) (20). The transcription level of *oxyR* was upregulated by 18-fold in the complemented strain compared with the wild-type strain (Fig. 3C). Accordingly, the mRNA level of *ccpA2* was significantly higher in the *oxyR*-complemented strain than that in the wild-type strain. Although the transcription levels of other antioxidant genes (*katE*, *ahpC1*, *ahpC2*, *ahpC3*, *ahpC4*, and *ahpF*) were significantly downregulated (Fig. 3C), the increased *ccpA2* expression level still conferred a higher antioxidant ability to the complemented strain than that of the wild-type strain (Fig. 3B). Therefore, of these genes, *ccpA2* was indicated to be the most important gene for adaptation to HHP and LT. Notably, CcpA2 is a homologue of CcpA in *Shewanella oneidensis* MR-1, which was positively regulated by the OxyR protein in *Shewanella oneidensis* MR-1 (OxyRso) and functions as a major H_2O_2-decomposing enzyme under anoxic conditions (21, 22). Recent findings showed that CcpA allowed bacteria to use H_2O_2 as a terminal electron acceptor to support anoxic respiration (23). AhpF, which is a flavoprotein with NADH:disulfide oxidoreductase and functions as an assistant to restore the disulfide in AhpC4 to its reduced form (24), was highly induced in the Δ*oxyR*c strain, indicating a demand for reducing equivalents of the strain for adaptation to HHP and LT. In addition to scavenger enzymes, the genes of the iron storage protein Dps were also upregulated in OE100. As Dps can sequester free iron inside the cell to prevent the excessive generation of harmful HO· by Fenton's reaction and shield DNA from damage (25), the upregulation of *dps* in OE100 suggested a need to minimize free iron during adaptation to HHP and LT.

In addition to an antioxidant defense system, an energy production system also contributes to adaptation to HHP and LT. WP3 has two sets of nitrate respiration systems, periplasmic dissimilatory nitrate reductase alpha (NAP-α) and NAP-β. A previous study demonstrated that both systems were functional, but NAP-α was a more efficient nitrate-reducing system (18). In addition, two sets of DMSO respiration systems were also identified in WP3, and both DMSO type I and type II systems were shown to be functional, but type I was more efficient for WP3 to thrive at 20 MPa and 4°C (26). In OE100, the NAP-β and DMSO type II systems showed higher expression levels in OE100 than in the WT, indicating that OE100 strengthens the less efficient respiration systems and thus produces more energy.

Moreover, the better adaptation of OE100 to HHP and LT can be partly due to repressed systems, including the SOS response and DNA repair systems. Although neither H_2O_2 nor O_2^- can damage DNA directly, H_2O_2 produces HO·, which can oxidize both base and ribose moieties of the DNA, giving rise to a wide variety of lesions and thus inducing the SOS response and activating the expression of DNA repair genes (24). Stress survival studies showed that an SOS-deficient mutant of *Listeria monocytogenes* was less resistant to H_2O_2 than the wild type (27). Compared to the WT, the key genes involved in the SOS response, *lexA* and *recA*, were downregulated in OE100, indicating that DNA damage under the tested conditions was not serious enough to activate the SOS response. In addition to *recA* and *lexA*, the transcription levels of some genes encoding DNA repair enzymes, including ImuA/B, MutT, and DNA polymerase IV, also showed downregulation, suggesting a low level of DNA damage that may be due to the enhanced antioxidation properties of OE100. Therefore, OE100 can redirect less energy utilization from proliferative processes to macromolecular processes and repair.

WP3 had two sets of flagellar systems, and a previous study showed that the expression of polar and lateral flagellar systems could respond to HHP and LT, respectively. The mutant lacking lateral flagella showed a significant decrease in growth at 4°C, which indicated that lateral flagella are important for the environmental adaptation of the strain at LT (28). Flagellins constitute the major extracellular part of the polar flagellum, which is responsible for swimming motility. In OE100, the major extracellular part of the polar flagellum of OE100 was lost during experimental evolution, leading to a decreased swimming motility of OE100 (see Fig. S3 in the supplemental material). Interestingly, out of 30 single-colony isolates that were randomly picked from 6 evolved populations, 6 strains were found to harbor the same deleted region in the polar flagellar gene *fliC1*, and all 6 of these isolates showed decreased swimming motility (Table S2). A trade-off between motility and oxidative stress resistance was also found for *Pseudomonas putida* KT2440, where the nonflagellated strain showed better resistance to paraquat-induced oxidative stress (29). Therefore, OE100 with impaired polar flagella can better cope with oxidative stress induced by HHP and LT. Moreover, a previous study demonstrated that the filamentous phage SW1 was active at 20 MPa and 4°C, and a significantly higher growth rate was observed for the phage-free strain than for wild-type strain WP3 at 20 MPa and 4°C (19, 30). Therefore, the downregulation of phage genes may partly contribute to the better growth ability of OE100. As the synthesis of both flagella and phage require plenty of energy, the repression of these systems showed that OE100 had more energy available to better adapt to HHP and LT.

Furthermore, a previous study showed that the overexpression of a single antioxidant enzyme of Kat, Ahp, or Dps could help bacteria to cope with many environmental stresses (e.g., cold, acid, heat, heavy metal, high salt concentrations, and UV) which can lead to oxidative stress (31–38), suggesting that antioxidant defense is a common adaptation strategy used by bacteria in response to environmental stressors other than HHP and LT.

In summary, this study confirmed the inherent relationship between antioxidant defense mechanisms and adaptation to HHP and LT, provides new scientific guidance for adaptation mechanisms of deep-sea bacteria, and provides an alternative method to obtain a bacterium with enhanced tolerance to HHP and LT by increasing its antioxidation capacity through experimental evolution. In the future, the protection of cells from oxidative stress damage should be taken into account when mimicking the cultivation of deep-sea bacteria or studying the diversity or characteristics of unculturable deep-sea microorganisms. Furthermore, this study provides insight into the pressure adaptation mechanism of *Shewanella*, and the transcriptomic data obtained from this study provide a valuable resource for further functional studies of the underlying molecular mechanisms in deep-sea bacteria.

MATERIALS AND METHODS

Experimental evolution. All bacterial strains and plasmids used in this study are listed in Table 4. The experimental evolution of WP3 under external H_2O_2 stress was performed as previously

TABLE 4 Bacterial strains and plasmids used in this study

Strain or plasmid	Description	Reference or source
Strains		
E. coli WM3064	Donor strain for conjugation; Δ*dapA*	46
S. piezotolerans WP3		
WT	Wild-type strain	Laboratory stock
OE100	Evolved strain derived from WP3	This study
WP3Δ4RE	Wild-type WP3 strain with 4 restriction enzyme gene deletions	19
WT/pSW2	WT with pSW2	This study
WP3Δ4RE/pSW2	WP3Δ4RE with pSW2	This study
Δ*oxyRc*	*oxyR* mutant derived from WP3Δ4RE	This study
Δ*oxyRc*/pSW2	Δ*oxyRc* strain with pSW2	This study
Δ*oxyRc*/*oxyR*	Δ*oxyRc* strain with pSW2-*oxyR*	This study
Δ*ccpA2*	*ccpA2* deletion mutant derived from WT	This study
Δ*ccpA2*/pSW2	Δ*ccpA2* with pSW2	This study
Δ*ccpA2*/*ccpA2*	Δ*ccpA2* with pSW2-*ccpA2*	This study
WT carrying *ccpA2*	WT with pSW2-*ccpA2*	This study
Plasmids		
pRE112	Chloramphenicol resistance; suicide plasmid with *sacB1* gene as a negative selection marker; used for gene deletion	47
pRE112-Δ*oxyRc*	pRE112 containing the PCR fragment for deleting *oxyR*	This study
pRE112-Δ*ccpA2*	pRE112 containing the PCR fragment for deleting *ccpA2*	This study
pSW2	Chloramphenicol resistance; generated from filamentous bacteriophage SW1; used for complementation	20
pSW2-*oxyR*	pSW2 containing *oxyR* for complementation	This study
pSW2-*ccpA2*	pSW2 containing *ccpA2* for complementation and overexpression	This study

described, with some modifications (39–41). Briefly, a single clonal isolate of *Shewanella piezotolerans* WP3 was used as the ancestor (WT) to 6 populations for experimental evolution. Six populations were propagated in 50 ml 2216E medium (5 g/liter tryptone, 1 g/liter yeast extract, and 34 g/liter NaCl). The cell cultures were aerobically grown at 20°C and at 200 rpm and were serially transferred to 50 ml 2216E medium with 0.4 mM H_2O_2 every 12 h with 1:100 dilutions. After 250 generations, the concentration of H_2O_2 added to the dilution medium was adjusted to 0.6 mM, and the populations evolved for 250 more generations. After a cumulative 500 generations of evolution, 6 single-colony isolates from each evolved population were randomly picked by plating and single-colony isolation. As one measure of evolving fitness, the endpoint growth level (culture density at the stationary phase) was measured in the cultures derived from each isolate. The strain with the highest endpoint culture density was selected and designated OE100.

Growth assay. The growth of the ancestral strain (WT) and the evolved strain (OE100) was examined with three replicates for each strain. For aerobic growth, the strains were cultured in 2216E broth in a rotary shaker (200 rpm) at 20°C or 4°C. For the anaerobic growth assay, serum bottles, each containing 100 ml of fresh medium, were anaerobically prepared by flushing with nitrogen gas through a butyl rubber stopper fixed with a metal seal to strip the dissolved oxygen prior to autoclave sterilization. To examine the growth of the strains at HHP, each culture was grown to log phase in 2216E medium at 1 atm and 20°C or 4°C in a rotary shaker. The log-phase cultures were diluted into the same medium to an optical density at 600 nm of 0.01. Aliquots of the diluted culture were injected into serum bottles containing 100 ml of anaerobic medium through the butyl rubber stopper. After brief shaking, 2.5-ml disposable plastic syringes were used to distribute the culture in 2-ml aliquots. The syringes with needles were stuck into rubber stoppers in a vinyl anaerobic airlock chamber (Coy Laboratory Products Inc., Grass Lake, MI, USA). The syringes were then incubated at a hydrostatic pressure of 20 MPa at 4°C or 20°C in stainless steel vessels (Feiyu Science and Technology Exploitation Co. Ltd., Nantong, China) that could be pressurized by using water and a hydraulic pump (5, 18, 26). These systems were equipped with quick-connect fittings for rapid decompression and recompression (achieving 20 MPa within 30 s). The cultures were held at 20 MPa and 20°C and at 20 MPa and 4°C for 24 h and 84 h, respectively.

H_2O_2 challenge assay. The response of the bacterial strains to H_2O_2 challenge was assessed by multiple approaches. A disc diffusion assay was employed to determine the impacts of H_2O_2 on bacterial lawns. Mid-log-phase cells were inoculated by 10-fold dilution into fresh broth and spread onto fresh 2216E plates (200 μl of culture; approximately 4×10^6 CFU). After 8 h, 6-mm-diameter paper discs loaded with 10 μl H_2O_2 (Sangon Biotech Co. Ltd., China) at concentrations of 1, 2, 4, and 8 M were placed onto the bacterial lawn. Plates were incubated at 20°C for 2 days. To determine the effect of H_2O_2 on the survival of cells, H_2O_2 at concentrations of 1, 2, 4, and 6 mM was added to the mid-log-phase cultures. After 20 min of incubation at 20°C, treatment was stopped by adding catalase (Worthington Biochemical Corporation, USA) at a concentration of 400 U/ml. The samples were diluted in a 3.4% NaCl solution and plated onto 2216E plates for counting viable colonies.

Colonies were counted after 2 days of incubation at 20°C. The results were expressed as percent survival, which is calculated by dividing the CFU per milliliter of surviving cells after 20 min by the CFU per milliliter of cells after 0 min. To examine the plating defects, cells at mid-log phase were adjusted to approximately 10^8 CFU/ml with fresh 2216E medium, followed by six 10-fold serial dilutions. Five microliters of each sample was spotted onto 2216E plates, and H_2O_2 was added at concentrations of 0.02, 0.04, and 0.08 mM. The plates were incubated for 2 days before being read. All experiments were repeated at least three times.

Swimming motility assay. The swimming motility assays were performed as previously described (42). Briefly, 1 μl of culture (mid-exponential phase) from each strain was placed onto swimming plates (2216E medium with 0.3% [wt/vol] agar). The plates were incubated at 20°C for 3 days. Motility was assessed by measuring the diameter of the colony. The assay was performed at least three independent times and in triplicate.

Genome sequencing. Cells of OE100 and WT bacteria growing in the exponential phase were harvested by centrifugation (12,000 $\times$ *g* for 3 min at 20°C), and the cell pellets were used for DNA extraction. High-molecular-weight DNA was extracted by using the phenol-chloroform method and sequenced by using the PacBio RS II sequencer with the P6-C4 sequencing reagent (Wuhan Institute of Biotechnology, China). We used the sequenced and annotated GenBank file of the genome of *S. piezotolerans* WP3 (GenBank accession no. NC_011566) as a reference and mapped the sequenced genomes.

Mutations in the evolved strain versus the ancestor were confirmed by the identification of SNPs and deletion-insertion polymorphisms (DIPs) by using Mauve2.4.0 (Darling Laboratory, University of Technology—Sydney). The presence of DIPs and suspected SNP sites in OE100 was verified by Sanger sequencing. The primers designed to amplify the PCR products for Sanger sequencing are listed in Table S1 in the supplemental material. Differences found in our ancestral strain from the reference WP3 genome were considered the "genetic property" of the ancestor.

Deletion mutagenesis and complementation. In-frame deletion mutagenesis of *oxyR* was performed as previously reported (26). The primers designed to amplify the PCR products for mutagenesis are summarized in Table 5. The PCR products were generated by using the DNA of OE100 as the templates with primers oxyRc-UF and oxyRc-UR. After digestion with the restriction enzymes SacI and KpnI, the treated fusion PCR products were ligated into the SacI and KpnI sites of suicide plasmid pRE112, resulting in mutagenesis vector pRE112-*oxyRc*. This vector was first introduced into *E. coli* WM3064 and then conjugated into WP3Δ4RE. Positive exconjugants were spread onto marine agar 2216E plates supplemented with 10% (wt/vol) sucrose. The chloramphenicol-sensitive and sucrose-resistant colonies were screened for the *oxyR*c deletion by PCR. The Δ*oxyR*c mutant was verified by sequencing of the mutated region. The same strategy was used to construct the Δ*ccpA2* strain.

Plasmid pSW2 was used for the genetic complementation of the mutant. The intact *oxyR* gene fragment was amplified from WT genomic DNA. The resulting PCR products were inserted into the shuttle vector pSW2. The Δ*oxyRc*/*oxyR* transformant was obtained by introducing recombinant plasmid pSW2-*oxyR* into the Δ*oxyR*c strain via conjugation. The same strategy was used to construct the complementing Δ*ccpA2*/*ccpA2* strain.

RNA sequencing and RNA-Seq data analysis. Total RNA from the WT and OE100 mutant strains at maximum growth yield under 20 MPa and 4°C was extracted by using TRIzol reagent according to the manufacturer's instructions (Invitrogen, Carlsbad, CA, USA). rRNA was removed by using a RiboMinus transcriptome isolation kit (Invitrogen, Carlsbad, CA, USA). Fragmentation buffer was added for interrupting mRNA into short fragments. Taking these short fragments as the templates, a random hexamer primer was used to synthesize the first-strand cDNA. The second-strand cDNA was synthesized by using buffer, dATPs, dGTPs, dCTPs, dUTPs, RNase H, and DNA polymerase I after the removal of deoxynucleoside triphosphates (dNTPs). Short fragments were purified with the QIAquick PCR purification kit (Qiagen, Hilden, Germany) and resolved with elution buffer (EB; 10 mM Tris-Cl, pH 8.5) for end repair and adding poly(A). After that, the short fragments were connected with sequencing adapters. The uracil-*N*-glycosylase (UNG) enzyme was then used to degrade the second-strand cDNA, and the product was purified by using a Mini Elute PCR purification kit (Qiagen, Hilden, Germany) before PCR amplification. RNA sequencing was performed on an Illumina HiSeq 2000 instrument (Illumina, San Diego, CA, USA) at the Beijing Genomics Institute (BGI) (China). A total of three independent biological replicates were prepared under each condition.

The clean data were trimmed from raw reads for further analysis by removing adapter sequences, low-quality reads (*Q* value of <20), ambiguous "N" nucleotides, and fragments of <20 bp. Unique sequences were mapped to the WP3 genome with SOAPaligner (soap2) (43). The uniquely mapped reads were collected and analyzed with the DEG-Seq package to identify the differentially expressed genes (estimation of gene expression levels based on the reads per kilobase per million [RPKM] values). Criteria of an FDR of <0.001 and the absolute value of a $\log_2$ fold change of ≥ 1 were used as the thresholds to judge the significance of the gene expression differences. The NOISeqBIO method was used to handle the biological replicates, and a probability of >0.8 and a $\log_2$ fold change of ≥ 1 were used as the thresholds to judge if the gene was differentially expressed under the two experimental conditions (44).

RT-qPCR. To validate the data generated by RNA-Seq, the expression levels of 10 randomly selected genes were quantified by using RT-qPCR. The primers were designed by using Primer Express software (Applied Biosystems, CA, USA) and are listed in Table 5. The amount of target was normalized to the reference gene swp2079 (45). A RT-qPCR assay of each biological replicate was carried out for three replicates, and the mean values and standard deviations were calculated for the relative RNA expression

TABLE 5 Primers used in this study

Oligonucleotide	Sequence (5′→3′)	Description
oxyRc-UF	GGCCGGTACCTTATTTTGTATGGAACAAAATAGACCATTTAGTCG	Gene deletion
oxyRc-UR	CTGTGAGCTCTGGTTAATTTACATCAAGAACAAAATTTTAATCGC	Gene deletion
oxyRF-C	TCGACTCGAGATGTCATTGGTAATCTGCTTTATGAAAC	Complementation
oxyRR-C	CGCGGATCCTTAATTATGTTGTTCAAGCAGCTTTTG	Complementation
ccpA2UF	TGCCGGTACCCGCTTGGTTGCTACTCCC	Gene deletion
ccpA2UR	ATAGTAAGGTTTGTCAATGTGCTC	Gene deletion
ccpA2DF	GACAAACCTTACTATGCCACGTCCTGTGCCTT	Gene deletion
ccpA2DR	GAACGAGCTCACAATACAGAGCCACACAACTGGTC	Gene deletion
ccpA2F-C	CCGCTCGAGATGAGCACATTGACAAACCTC	Complementation
ccpA2R-C	CGCGGATCCCTAGTTAGCAAAAGGCACAG	Complementation
oxyR-F	GCAATTGGTATTAAAAACCCTAAATAC	*oxyR* sequencing
oxyR-R	AAGGATGCCTTGAGAAATCTATG	*oxyR* sequencing
katF	CCTGCGTGACGGGATTAAGT	RT-qPCR
katR	CGGGTTGCGCTTTTGG	RT-qPCR
ahpC1F	CGCATGATCGACGCACTTC	RT-qPCR
ahpC1R	CCAACCAGCAGGACAAACATC	RT-qPCR
ahpC2F	CACTTCTAAGCGACGAAGACCAT	RT-qPCR
ahpC2R	AATTTCTTCTCCCCCCAAACA	RT-qPCR
ahpC3F	CCAAACTCACTGCCGGAAA	RT-qPCR
ahpC3R	GCACCAGCCACCACGATAG	RT-qPCR
ahpC4F	CCCAACTGGCGCAATCAC	RT-qPCR
ahpC4R	GCGCTAAGCCATCTTCTTCAA	RT-qPCR
ahpFF	AACGTACCGGGTGAGCAAGA	RT-qPCR
ahpFR	TCACAATGTGGGCAATAAGCA	RT-qPCR
ccpA1F	ACTCGAGAACGAATTGCACAAG	RT-qPCR
ccpA1R	CGGCGCGATAGGATGGT	RT-qPCR
ccpA2F	GGGTTGGCCCAGTTTTGG	RT-qPCR
ccpA2R	GACCGCCTGCTTGCTCTTTA	RT-qPCR
ccpA3F	GCCTCATGCCATGTGCAA	RT-qPCR
ccpA3R	ACCAATACTCAAGCGACGAGAGT	RT-qPCR
ccpA4F	TGCCCCAAGCCGCTATC	RT-qPCR
ccpA4R	CAATAAATGCAGCCCAAATCC	RT-qPCR
gpxF	GGTGCTCAAGAAAAAGGCGATA	RT-qPCR
gpxR	CCCAAAGTTGAGTTCGCAAAA	RT-qPCR
dpsF	CCGCTGCTTGGTACCATTG	RT-qPCR
dpsR	CGCTAACAGCGATGGGAAGT	RT-qPCR
oxyF	GGCGAAGAGGTGGTGTTACG	RT-qPCR
oxyR	GCTCGACCAAATCATCCACATC	RT-qPCR
swp2079F	TTAAGGCAATGGAAGCTGCAT	RT-qPCR
swp2079R	CGTCTTTACCCGTTAATGATACGA	RT-qPCR
SWP_03625F	GCGGAAGAAAACAGCGATAAA	RNA-Seq validation
SWP_03625R	TGCTCACCAATACCAGCTTCTG	RNA-Seq validation
SWP_06535F	CGAGGGCTATGCTCGTCTCTT	RNA-Seq validation
SWP_06535R	TTGCCAGAGGCGCTTTTT	RNA-Seq validation
SWP_11550F	TTTCACCGACTGAATACAATTTAGCT	RNA-Seq validation
SWP_11550R	CAAGCCCAAAGACCTGCAAA	RNA-Seq validation
SWP_11565F	ACAAGTGCTGTTGAGTTTCTAAAGGA	RNA-Seq validation
SWP_11565R	CCACCGCACCAAATAGCATA	RNA-Seq validation
SWP_11570F	TCAGAAACAGGGTCTACTGCAGTT	RNA-Seq validation
SWP_11570R	ATCGACTGATTTTTGAGGCTTTAAG	RNA-Seq validation
SWP_18205F	TGCCGAGCAAGCTTTTGC	RNA-Seq validation
SWP_18205R	TGCTCTGCTGAAACCTTACCATT	RNA-Seq validation
SWP_20695F	TGAGCATGCCACTGAGTATGG	RNA-Seq validation
SWP_20695R	TTGCGCAGTACATTGAACTCAA	RNA-Seq validation
SWP_20720F	AAACATGACCGCAGGCAGTAG	RNA-Seq validation
SWP_20720R	GCAAGCCAGAATCGGTAACG	RNA-Seq validation
SWP_21995F	GGCAGAGACATTCCAAACTCTAGAA	RNA-Seq validation
SWP_21995R	GGCAGTTGATATTGCGCTTGA	RNA-Seq validation

levels. The RT-qPCR $\log_2$ ratio values were plotted against the RNA-Seq data $\log_2$ values, and the correlation coefficients (R^2) between these two data sets were calculated.

In the assessment of the effect of reduced levels of OxyR on the expression levels of various H_2O_2-scavenging genes, the expression levels of target genes in the Δ*oxyR*c strain carrying pSW2 and the Δ*oxyR*c/*oxyR* strain were normalized relative to those in WP3Δ4RE/pSW2.

Accession number(s). The RNA-Seq raw reads were deposited in the Gene Expression Omnibus (GEO) database of the NCBI with accession no. GSE99297.

SUPPLEMENTAL MATERIAL

Supplemental material for this article may be found at https://doi.org/10.1128/AEM.02342-17.

SUPPLEMENTAL FILE 1, PDF file, 1.0 MB.

ACKNOWLEDGMENTS

We thank Xiaopan Ma for the valuable discussions about our data.

This work was financially supported by the National Natural Science Foundation of China (grant no. 31290232 and 41530967) and the China Ocean Mineral Resources R&D Association (grant no. DY125-22-04).

REFERENCES

1. Oger PM, Jebbar M. 2010. The many ways of coping with pressure. Res Microbiol 161:799–809. https://doi.org/10.1016/j.resmic.2010.09.017.
2. Xiao X, Zhang Y. 2014. Life in extreme environments: approaches to study life-environment co-evolutionary strategies. Sci China Earth Sci 57:869–877. https://doi.org/10.1007/s11430-014-4858-8.
3. De Maayer P, Anderson D, Cary C, Cowan DA. 2014. Some like it cold: understanding the survival strategies of psychrophiles. EMBO Rep 15:508–517. https://doi.org/10.1002/embr.201338170.
4. Green J, Paget MS. 2004. Bacterial redox sensors. Nat Rev Microbiol 2:954–966. https://doi.org/10.1038/nrmicro1022.
5. Zhang Y, Li X, Bartlett DH, Xiao X. 2015. Current developments in marine microbiology: high-pressure biotechnology and the genetic engineering of piezophiles. Curr Opin Biotech 33:157–164. https://doi.org/10.1016/j.copbio.2015.02.013.
6. Ambily Nath IV, Loka Bharathi PA. 2011. Diversity in transcripts and translational pattern of stress proteins in marine extremophiles. Extremophiles 15:129–153. https://doi.org/10.1007/s00792-010-0348-x.
7. Shah J, Desai PT, Chen D, Stevens JR, Weimer BC. 2013. Preadaptation to cold stress in *Salmonella enterica* serovar Typhimurium increases survival during subsequent acid stress exposure. Appl Environ Microbiol 79:7281–7289. https://doi.org/10.1128/AEM.02621-13.
8. Garnier M, Matamoros S, Chevret D, Pilet MF, Leroi F, Tresse O. 2010. Adaptation to cold and proteomic responses of the psychrotrophic biopreservative *Lactococcus piscium* strain CNCM I-4031. Appl Environ Microbiol 76:8011–8018. https://doi.org/10.1128/AEM.01331-10.
9. Marietou A, Nguyen AT, Allen EE, Bartlett DH. 2014. Adaptive laboratory evolution of *Escherichia coli* K-12 MG1655 for growth at high hydrostatic pressure. Front Microbiol 5:749. https://doi.org/10.3389/fmicb.2014.00749.
10. Aertsen A, De Spiegeleer P, Vanoirbeek K, Lavilla M, Michiels CW. 2005. Induction of oxidative stress by high hydrostatic pressure in *Escherichia coli*. Appl Environ Microbiol 71:2226–2231. https://doi.org/10.1128/AEM.71.5.2226-2231.2005.
11. Kish A, Griffin PL, Rogers KL, Fogel ML, Hemley RJ, Steele A. 2012. High-pressure tolerance in *Halobacterium salinarum* NRC-1 and other non-piezophilic prokaryotes. Extremophiles 16:355–361. https://doi.org/10.1007/s00792-011-0418-8.
12. Bravim F, Mota MM, Fernandes AA, Fernandes PM. 2016. High hydrostatic pressure leads to free radicals accumulation in yeast cells triggering oxidative stress. FEMS Yeast Res 16:fow052. https://doi.org/10.1093/femsyr/fow052.
13. Xiao X, Wang P, Zeng X, Bartlett DH, Wang F. 2007. *Shewanella psychrophila* sp. nov. and *Shewanella piezotolerans* sp. nov., isolated from west Pacific deep-sea sediment. Int J Syst Evol Microbiol 57:60–65. https://doi.org/10.1099/ijs.0.64500-0.
14. Imlay JA. 2015. Transcription factors that defend bacteria against reactive oxygen species. Annu Rev Microbiol 69:93–108. https://doi.org/10.1146/annurev-micro-091014-104322.
15. Berkovitch F, Nicolet Y, Wan JT, Jarrett JT, Drennan CL. 2004. Crystal structure of biotin synthase, an S-adenosylmethionine-dependent radical enzyme. Science 303:76–79. https://doi.org/10.1126/science.1088493.
16. Conrad TM, Lewis NE, Palsson BØ. 2011. Microbial laboratory evolution in the era of genome-scale science. Mol Syst Biol 7:509. https://doi.org/10.1038/msb.2011.42.
17. Marritt SJ, Lowe TG, Bye J, McMillan DGG, Shi L, Fredrickson J, Zachara J, Richardson DJ, Cheesman MR, Jeuken LJC, Butt JN. 2012. A functional description of CymA, an electron-transfer hub supporting anaerobic respiratory flexibility in *Shewanella*. Biochem J 444:465–474. https://doi.org/10.1042/BJ20120197.
18. Chen Y, Wang F, Xu J, Mehmood MA, Xiao X. 2011. Physiological and evolutionary studies of NAP systems in *Shewanella piezotolerans* WP3. ISME J 5:843–855. https://doi.org/10.1038/ismej.2010.182.
19. Jian H, Xiong L, Xu G, Xiao X, Wang F. 2016. Long 5′ untranslated regions regulate the RNA stability of the deep-sea filamentous phage SW1. Sci Rep 6:21908. https://doi.org/10.1038/srep21908.
20. Yang XW, Jian HH, Wang FP. 2015. pSW2, a novel low-temperature-inducible gene expression vector based on a filamentous phage of the deep-sea bacterium *Shewanella piezotolerans* WP3. Appl Environ Microbiol 81:5519–5526. https://doi.org/10.1128/AEM.00906-15.
21. Jiang YM, Dong YY, Luo QX, Li N, Wu GF, Gao HC. 2014. Protection from oxidative stress relies mainly on derepression of OxyR-dependent KatB and Dps in *Shewanella oneidensis*. J Bacteriol 196:445–458. https://doi.org/10.1128/JB.01077-13.
22. Schutz B, Seidel J, Sturm G, Einsle O, Gescher J. 2011. Investigation of the electron transport chain to and the catalytic activity of the diheme cytochrome *c* peroxidase CcpA of *Shewanella oneidensis*. Appl Environ Microbiol 77:6172–6180. https://doi.org/10.1128/AEM.00606-11.
23. Kaya A, Mariotti M, Gladyshev VN. 2017. Cytochrome *c* peroxidase facilitates the beneficial use of H_2O_2 in prokaryotes. Proc Natl Acad Sci U S A 114:8678–8680. https://doi.org/10.1073/pnas.1710943114.
24. Imlay JA. 2013. The molecular mechanisms and physiological consequences of oxidative stress: lessons from a model bacterium. Nat Rev Microbiol 11:443–454. https://doi.org/10.1038/nrmicro3032.
25. Calhoun LN, Kwon YM. 2011. Structure, function and regulation of the DNA-binding protein Dps and its role in acid and oxidative stress resistance in *Escherichia coli*: a review. J Appl Microbiol 110:375–386. https://doi.org/10.1111/j.1365-2672.2010.04890.x.
26. Xiong L, Jian H, Zhang Y, Xiao X. 2016. The two sets of DMSO respiratory systems of *Shewanella piezotolerans* WP3 are involved in deep sea environmental adaptation. Front Microbiol 7:1418. https://doi.org/10.3389/fmicb.2016.01418.
27. van der Veen S, van Schalkwijk S, Molenaar D, de Vos WM, Abee T, Wells-Bennik MHJ. 2010. The SOS response of *Listeria monocytogenes* is involved in stress resistance and mutagenesis. Microbiology 156:374–384. https://doi.org/10.1099/mic.0.035196-0.
28. Wang F, Wang J, Jian H, Zhang B, Li S, Wang F, Zeng X, Gao L, Bartlett DH, Yu J, Hu S, Xiao X. 2008. Environmental adaptation: genomic analysis of the piezotolerant and psychrotolerant deep-see iron reducing bacterium *Shewanella piezotolerans* WP3. PLoS One 3:e1937. https://doi.org/10.1371/journal.pone.0001937.
29. Martinez-Garcia E, Nikel PI, Chavarria M, de Lorenzo V. 2014. The metabolic cost of flagellar motion in *Pseudomonas putida* KT2440. Environ Microbiol 16:291–303. https://doi.org/10.1111/1462-2920.12309.
30. Wang F, Wang FP, Li Q, Xiao X. 2007. A novel filamentous phage from the deep-sea bacterium *Shewanella piezotolerans* WP3 is induced at low temperature. J Bacteriol 189:7151–7153. https://doi.org/10.1128/JB.00569-07.
31. Goto S, Kawamoto J, Sato SB, Iki T, Watanabe I, Kudo K, Esaki N, Kurihara T. 2015. Alkyl hydroperoxide reductase enhances the growth of *Leuconostoc mesenteroides* lactic acid bacteria at low temperatures. AMB Express 5:11. https://doi.org/10.1186/s13568-015-0098-3.
32. Smirnova GV, Muzyka NG, Oktyabrsky ON. 2000. The role of antioxidant

enzymes in response of *Escherichia coli* to osmotic upshift. FEMS Microbiol Lett 186:209–213. https://doi.org/10.1111/j.1574-6968.2000.tb09106.x.
33. Noor R. 2015. Mechanism to control the cell lysis and the cell survival strategy in stationary phase under heat stress. Springerplus 4:599. https://doi.org/10.1186/s40064-015-1415-7.
34. den Besten HM, Effraimidou S, Abee T. 2013. Catalase activity as a biomarker for mild-stress-induced robustness in *Bacillus weihenstephanensis*. Appl Environ Microbiol 79:57–62. https://doi.org/10.1128/AEM.02282-12.
35. Rothe M, Alpert C, Engst W, Musiol S, Loh G, Blaut M. 2012. Impact of nutritional factors on the proteome of intestinal *Escherichia coli*: induction of OxyR-dependent proteins AhpF and Dps by a lactose-rich diet. Appl Environ Microbiol 78:3580–3591. https://doi.org/10.1128/AEM.00244-12.
36. Mishra Y, Chaurasia N, Rai LC. 2009. AhpC (alkyl hydroperoxide reductase) from *Anabaena* sp PCC 7120 protects *Escherichia coli* from multiple abiotic stresses. Biochem Biophys Res Commun 381:606–611. https://doi.org/10.1016/j.bbrc.2009.02.100.
37. Choi SH, Baumler DJ, Kaspar CW. 2000. Contribution of *dps* to acid stress tolerance and oxidative stress tolerance in *Escherichia coli* O157:H7. Appl Environ Microbiol 66:3911–3916. https://doi.org/10.1128/AEM.66.9.3911-3916.2000.
38. Chiancone E, Ceci P. 2010. The multifaceted capacity of Dps proteins to combat bacterial stress conditions: detoxification of iron and hydrogen peroxide and DNA binding. Biochim Biophys Acta 1800:798–805. https://doi.org/10.1016/j.bbagen.2010.01.013.
39. Zhou A, Baidoo E, He Z, Mukhopadhyay A, Baumohl JK, Benke P, Joachimiak MP, Xie M, Song R, Arkin AP, Hazen TC, Keasling JD, Wall JD, Stahl DA, Zhou J. 2013. Characterization of NaCl tolerance in *Desulfovibrio vulgaris* Hildenborough through experimental evolution. ISME J 7:1790–1802. https://doi.org/10.1038/ismej.2013.60.
40. Harden MM, He A, Creamer K, Clark MW, Hamdallah I, Martinez KA, II, Kresslein RL, Bush SP, Slonczewski JL. 2015. Acid-adapted strains of *Escherichia coli* K-12 obtained by experimental evolution. Appl Environ Microbiol 81:1932–1941. https://doi.org/10.1128/AEM.03494-14.
41. Dragosits M, Mozhayskiy V, Quinones-Soto S, Park J, Tagkopoulos I. 2013. Evolutionary potential, cross-stress behavior and the genetic basis of acquired stress resistance in *Escherichia coli*. Mol Syst Biol 9:643. https://doi.org/10.1038/msb.2012.76.
42. Jian H, Xiao X, Wanga F. 2013. Role of filamentous phage SW1 in regulating the lateral flagella of *Shewanella piezotolerans* strain WP3 at low temperatures. Appl Environ Microbiol 79:7101–7109. https://doi.org/10.1128/AEM.01675-13.
43. Li RQ, Li YR, Kristiansen K, Wang J. 2008. SOAP: short oligonucleotide alignment program. Bioinformatics 24:713–714. https://doi.org/10.1093/bioinformatics/btn025.
44. Tarazona S, Furió-Tarí P, Turrà D, Pietro AD, Nueda MJ, Ferrer A, Conesa A. 2015. Data quality aware analysis of differential expression in RNA-seq with NOISeq R/Bioc package. Nucleic Acids Res 43:e140. https://doi.org/10.1093/nar/gkv711.
45. Yang XW, He Y, Xu J, Xiao X, Wang FP. 2013. The regulatory role of ferric uptake regulator (Fur) during anaerobic respiration of *Shewanella piezotolerans* WP3. PLoS One 8:e75588. https://doi.org/10.1371/journal.pone.0075588.
46. Gao HC, Yang ZMK, Wu LY, Thompson DK, Zhou JZ. 2006. Global transcriptome analysis of the cold shock response of *Shewanella oneidensis* MR-1 and mutational analysis of its classical cold shock proteins. J Bacteriol 188:4560–4569. https://doi.org/10.1128/JB.01908-05.
47. Edwards RA, Keller LH, Schifferli DM. 1998. Improved allelic exchange vectors and their use to analyze 987P fimbria gene expression. Gene 207:149–157. https://doi.org/10.1016/S0378-1119(97)00619-7.